Space Weather

RESEARCH ARTICLE
10.1029/2025SW004681

High Voltage DC Active Current Injection to Simulate Geomagnetically Induced Currents in New Zealand

Soren Subritzky[1], Andrew Lapthorn[1], Stewart Hardie[1], Paul Agger[1], Mike Dalzell[2], Mark A. Clilverd[3], Neil Cobbett[3], Ciaran Beggan[4], Juliane Hübert[4], Eliot Eaton[4], James B. Brundell[5], and Craig J. Rodger[5]

[1]Department of Electrical and Computer Engineering, University of Canterbury, Christchurch, New Zealand, [2]Transpower New Zealand Limited, Wellington, New Zealand, [3]British Antarctic Survey, Cambridge, UK, [4]British Geological Survey, Edinburgh, UK, [5]Department of Physics, University of Otago, Dunedin, New Zealand

Abstract This study investigates the effects of geomagnetically induced currents (GIC) on New Zealand's electrical infrastructure via an intentional ground injection of direct current (DC) from a high voltage DC converter station. GIC manifests as quasi-DC currents within power systems, potentially causing transformer saturation, increased reactive power demand, elevated harmonics, and transformer overloading. In January 2023, with support from Transpower, we utilized New Zealand's high voltage DC link to inject current directly into the ground at Haywards substation in Wellington, North island. This allowed us to monitor the effects of half-cycle saturation of two 216 MVA, 220/110 kV autotransformers. Over 9 days, six injection tests were conducted, each lasting between one and 2 hours, with peak ground injection current reaching approximately 621 A, corresponding to 35 A measured to flow through one of the transformers on site. The saturation threshold of the transformer was measured to be around 20 A. Analysis of power quality measurements revealed a clear correlation between even total harmonic distortion and DC current, along with corresponding increases in acoustic sound and vibration levels. There was strong agreement between differential magnetometer (DMM) and transformer measurements of DC current. Variations in very low frequency radio harmonic observations were correlated with temporal variations in ground current. These findings provide valuable insights into the impact of GICs on in-service equipment and inform grid operators on potential mitigation strategies.

Plain Language Summary This study investigates the effects of geomagnetically induced currents (GIC) on operational power transformers and the surrounding electrical network. High levels of GIC can be harmful to power transformers potentially causing unwanted power outages and in the worst case blackouts of entire grids. In this experiment we injected GIC into two transformers at a substation in Wellington, New Zealand. Measurements were made of the transformers' voltage, current, noise and vibration levels alongside the surrounding radio waves and magnetic field in the power-lines. Analysis of the transformers' voltage and current found a reduction in power quality alongside corresponding increases in sound and vibration levels. The variations in the radio waves corresponded well with the injected GIC and the magnetic field measurements in the power lines corresponded well with the transformer measurements. These findings provide valuable insights into the impact of GICs on in-service equipment and inform grid operators on potential mitigation strategies.

Key Points:

- Direct current injection test carried out at a New Zealand substation to study geomagnetically induced current impacts on power transformers
- Power quality, differential magnetometer, and very low frequency radio measurements were taken during the experiment
- Evidence of half-cycle transformer saturation was found through an enhancement in even harmonics alongside vibration and sound levels

Supporting Information:

Supporting Information may be found in the online version of this article.

Correspondence to:

S. Subritzky,
soren.subritzky@pg.canterbury.ac.nz

Citation:

Subritzky, S., Lapthorn, A., Hardie, S., Agger, P., Dalzell, M., Clilverd, M. A., et al. (2026). High voltage DC active current injection to simulate geomagnetically induced currents in New Zealand. *Space Weather*, *24*, e2025SW004681. https://doi.org/10.1029/2025SW004681

Received 20 AUG 2025
Accepted 3 MAR 2026

Author Contributions:

Conceptualization: Soren Subritzky, Andrew Lapthorn, Mike Dalzell, Craig J. Rodger
Data curation: Soren Subritzky, Andrew Lapthorn, Stewart Hardie, Mike Dalzell, Mark A. Clilverd, Neil Cobbett, Ciaran Beggan, Juliane Hübert, Eliot Eaton
Formal analysis: Soren Subritzky, Andrew Lapthorn, Stewart Hardie, Mark A. Clilverd, Neil Cobbett, Ciaran Beggan, Juliane Hübert, Eliot Eaton, James B. Brundell
Funding acquisition: Andrew Lapthorn, Craig J. Rodger

1. Introduction

The importance of electricity in modern society cannot be overstated. Since the widespread adoption of electricity, developed nations have experienced significant growth in wealth and prosperity. A study by Ferguson et al. (2000) examining the relationship between electricity use and economic development in over 100 countries —representing more than 99% of the global economy—found that wealthier nations show a stronger correlation between electricity consumption and wealth creation compared to developing countries. Furthermore, for the global economy as a whole, the correlation between electricity use and wealth creation is stronger than that between total energy use and wealth.

The operation and maintenance of electrical networks are complex and costly tasks, with the responsibility for ensuring the reliable operation of the electricity system resting primarily on the System Operator. Large-scale blackouts can have significant direct and indirect economic and national security consequences. Although large cascading blackouts in power transmission systems are relatively rare, their potential impact makes understanding the risks associated with such events a high priority (Newman et al., 2011; Yamashita et al., 2008).

Investigation: Soren Subritzky, Andrew Lapthorn, Stewart Hardie, Paul Agger, Mark A. Clilverd, Neil Cobbett, Ciaran Beggan, Juliane Hübert, Eliot Eaton, James B. Brundell
Methodology: Soren Subritzky, Andrew Lapthorn, Stewart Hardie, Mark A. Clilverd, Ciaran Beggan, Juliane Hübert, Eliot Eaton
Project administration: Andrew Lapthorn, Mike Dalzell, Craig J. Rodger
Resources: Andrew Lapthorn, Paul Agger, Mike Dalzell, Craig J. Rodger
Software: Soren Subritzky, Stewart Hardie, Mark A. Clilverd, Ciaran Beggan, Juliane Hübert, Eliot Eaton
Supervision: Andrew Lapthorn, Paul Agger, Mike Dalzell
Validation: Soren Subritzky, Andrew Lapthorn, Stewart Hardie, Mike Dalzell, Mark A. Clilverd, Neil Cobbett, Ciaran Beggan, Juliane Hübert, Eliot Eaton
Visualization: Soren Subritzky, Andrew Lapthorn, Stewart Hardie, Mark A. Clilverd, Ciaran Beggan, Juliane Hübert, Eliot Eaton, Craig J. Rodger
Writing – original draft: Soren Subritzky, Andrew Lapthorn, Stewart Hardie, Mark A. Clilverd, Ciaran Beggan, Juliane Hübert
Writing – review & editing: Soren Subritzky, Andrew Lapthorn, Stewart Hardie, Mark A. Clilverd, Ciaran Beggan, Juliane Hübert, Eliot Eaton, Craig J. Rodger

There are numerous risks to the security of electricity supply, stemming from both natural and man-made hazards. It is crucial to have adequate planning in place to address these risks. Natural disasters, such as earthquakes, volcanic eruptions, and flooding, can have far-reaching effects. In New Zealand, planning measures are already in place to manage these natural disasters; however, recent research has increasingly focused on the potential impacts of space weather.

Several noteworthy space weather events have occurred in the past. The March 1989 geomagnetic storm caused the failure of the Quebec power grid (Bolduc, 2002) and damaged transformers in the United Kingdom (Erinmez et al., 2002) and United States (Boteler, 2019). In October 2003, another geomagnetic disturbance resulted in a short-term blackout affecting 50,000 customers in Sweden (Pulkkinen et al., 2005). One of the largest recorded events, the "Carrington" event of 1859, created auroras visible as far as 23° from the Earth's equator and created widespread problems for the telegraph: the new technology of the time (Tsurutani et al., 2003). It appears that storms as powerful as the Carrington event are possible in the present time; for example, the July 2012 coronal mass ejection narrowly missed Earth (Ngwira et al., 2013).

Geomagnetically induced currents (GIC) present a significant threat to the reliable operation of power systems. These currents, caused by geoeffective coronal mass ejections and their interaction with the Earth's magnetic field, manifest as quasi-direct current (DC) in a power system and can severely disrupt electrical infrastructure, leading to costly damage and service interruptions. Understanding the characteristics, mechanisms, and effects of GIC is essential for designing resilient power systems and developing effective mitigation strategies.

Under DC excitation, transformers can enter a state known as half-cycle saturation, which involves a DC offset in the transformer flux, leading to a range of issues as outlined by the IEEE standard for GIC (IEEE, 2024). These include increased reactive power demand, losses, elevated sound levels, and vibrations in the transformer tank. Due to the asymmetrical nature of half-cycle saturation, both even and odd AC harmonics are produced. The rise in harmonic levels can impact ancillary equipment, resulting in relay misoperations, overstressed capacitor banks, and overheating of generator rotors.

The transformers' susceptibility to GIC depends strongly on its core construction. Core form transformers have their outer winding's surround the core (e.g., three-phase three-limb core) so the flux return path is through the high reluctance air whereas in shell form transformers (e.g., three-phase five-limb) the core surrounds the outer winding's so the flux return path is through the low reluctance core. Due to the higher reluctance return path core form transformers are more resilient to half-cycle saturation than shell form as demonstrated by Teh et al. (2022).

Currently, there are very few studies that examine the effects of DC on in-service power transformers, with most research conducted in highly controlled environments. For instance, He et al. (2012) investigated the vibration and noise characteristics of an AC transformer caused by high-voltage direct current (HVDC) monopole operation. During this testing, DC bias experiments were conducted on 500 kV power transformers in both transformer factory and substation settings, revealing an increase in vibration and audible noise during the DC injection. Zeng et al. (2011) studied an HVDC transmission system in Guangdong, China, and found that during DC injection, there was a significant rise in voltage distortion and audible noise. R. Girgis and Ko (1992) has performed extensive research on transformers under DC excitation, focusing in detail on the effects of GIC, including reactive power demand, thermal characteristics, harmonics, and noise characteristics (R. Girgis & Ko, 1992; R. Girgis & Vedante, 2012, 2013; R. S. Girgis et al., 2019). Much of this research has been incorporated into the IEEE standard for power transformer GIC capability (IEEE, 2024).

In this study, we introduce a pioneering experiment conducted in New Zealand, utilizing a 1200 MW HVDC converter station to inject DC into the ground, thereby simulating geomagnetically induced currents. Between 21 and 29 January 2023, with the assistance of Transpower New Zealand Ltd (New Zealand's grid owner and operator) and the Solar Tsunamis research program, we successfully utilized New Zealand's HVDC link to directly introduce DC into the ground at Haywards substation. Some of the current flowed through the transformers and onto the AC transmission lines connected to Haywards substation. Our objective was to observe the impact on two 216 MVA, 220/110 kV autotransformers, as well as to monitor the associated transmission lines. We performed direct measurements on two operational power transformers, assessing parameters such as power quality, audible noise, and vibration. Additionally, we conducted indirect measurements of the substation through very low frequency (VLF) monitoring and differential magnetometer measurements (DMM) of the surrounding transmission lines. Over a period of 9 days, we conducted six injection tests, each lasting between one and 2 hours.

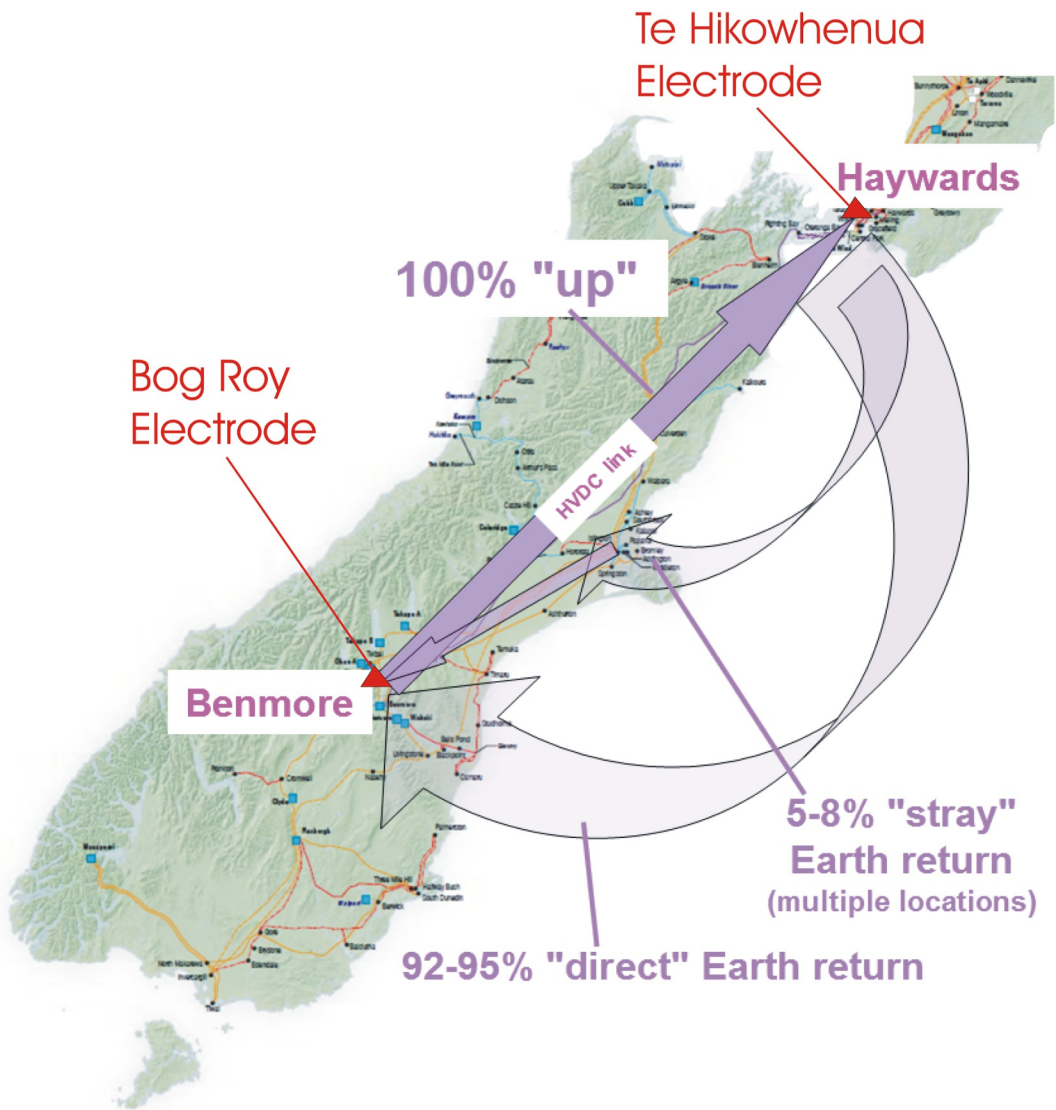

Figure 1. Diagram outlining stray Earth return currents (Mac Manus et al., 2017).

The outcomes of this research provide valuable insights for grid operators regarding the impact of GIC on in-service equipment.

In the following section, we describe the experimental methodology, including the operation of the HVDC link and the equipment used for the various measurements. The results of these measurements are then presented and discussed, followed by concluding remarks.

2. Methods

In this section is an overview of the testing methodology and the experimental setup.

2.1. The HVDC Converter Station and Experiment Setup

New Zealand's electrical transmission network comprises two isolated AC grids, one on the North Island and the other on the South Island. The only connection between these two islands is through the HVDC link, depicted by the purple line in Figure 1. The link provides security of supply to the New Zealand electricity market by allowing power transfer from the multiple hydroelectric power stations found in the South Island to the main load centers in the North Island. The HVDC link has two converter stations, one at the Benmore Hydroelectric Power Station,

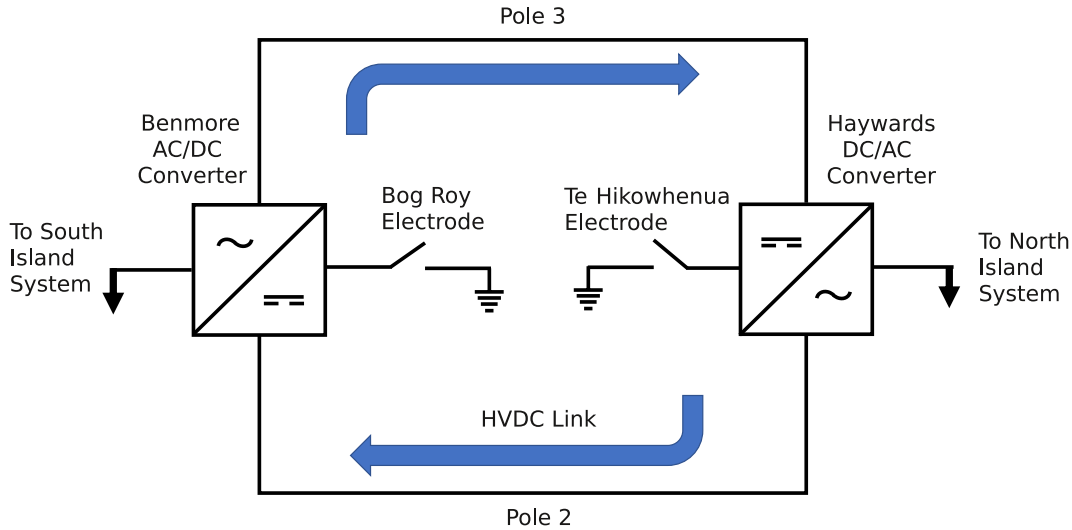

Figure 2. Simplified single line diagram of the high-voltage direct current links and their connections to the AC grids at Benmore (South island) and Haywards (North Island).

situated on the Waitaki River in Canterbury on the South Island and the other at the Haywards Substation in Lower Hutt, Wellington, on the North Island. The link spans a total distance of 610 km, which includes 570 km of overhead lines and 40 km of undersea cable crossing Cook Strait. Currently, the link has a capacity of 1,200 MW (Mac Manus et al., 2017).

The HVDC link consists of a thyristor-based, line commutated converter bipolar topology, and as such, can operate in either bipole mode (poles 2 and 3–pole 1 was decommissioned in 2012), where the current is shared equally between the two transmission conductors or in monopole Earth-return mode where the current returns through the Earth Electrode Stations, Te Hikowhenua Electrode at Makara near Haywards and Bog Roy Electrode at Benmore (Figure 2).

When the HVDC link operates in Earth-return mode, a small portion of the Earth-return current can flow from the Te Hikowhenua Electrode at Makara into the South Island power grid through multiple earthing points in substations across the island, as shown in Figure 1. This "stray" Earth return current flows across transmission lines to the Bog Roy Electrode at Benmore (Mac Manus et al., 2017). The effect of these stray currents on the power system is not too dissimilar to GIC. To mitigate against the Earth return currents, Transpower has installed neutral earthing resistors on many, but not all, power transformers in the New Zealand power network, which have earthed high voltage windings.

To simulate GIC in the network, the HVDC link was operated in Earth-return mode, and the station ground at Haywards was connected to the Earth grid. This configuration results in the converter's current being directly injected into the ground via the station's Earth grid. The injection periods were controlled by Transpower and were based on the market conditions at the time and maintenance schedule for the HVDC link. When the power demand in the North or South Island goes below a certain threshold (200 MW) the HVDC link operates in Earth-return mode and depending on the maintenance schedule the current can be distributed differently.

For periods during the experiment, the line between Haywards and Makara was taken out of service (Station Ground Only). This caused the converter current to flow through the station ground instead of the Te Hikowhenua electrode. The Te Hikowhenua electrode and station ground were in parallel when the line was in service (Electrode and Station Ground in Parallel), causing the DC to be shared during normal operation.

The station ground forms a circuit with earthed power transformers and other equipment causing the DC current to be distributed throughout the substation. This creates the test conditions for GIC. Table 1 shows a summary of the events during the experiment. Throughout the experiment, there were six separate DC injections in total.

Table 1
Summary of the DC Injection Events

Date	Time (NZST)	Duration (mins)	Peak Earth grid current (A)	Peak current through T1 (A)	Notes
21/01/2023	7:05	73	441	20	Station Ground Only
22/01/2023	13:35	127	392	21	Station Ground Only
26/01/2023	17:09	83	374	15	Electrode and station ground in parallel
26/01/2023	21:08	112	508	19	Electrode and station ground in parallel
28/01/2023	11:03	82	605	35	Station Ground Only, T5 out of service
29/01/2023	19:39	121	621	28	Station Ground Only

Note. Time is in New Zealand Standard Time (NZST = UTC + 13 hr in summer months).

2.2. Transformer Monitoring

Two transformers were monitored during the experiment, designated as Haywards T1 and Haywards T5 (See Figure S2 in Supporting Information S1). They are 216 MVA 220/110 kV autotransformers. The core construction is a three-phase, three-limb design, and as such are relatively resilient to DC (and GIC) (Teh et al., 2022).

Voltage, current and power waveforms across the transformer were monitored via multiple power quality meters at both the 110 and 220 kV windings. The sampling interval was every 3 seconds, with a 200 ms snapshot of the waveforms captured every minute. DC was measured using LEM current sensors on the transformer neutral and was monitored by Transpower through the Supervisory Control and Data Acquisition system. For more information on the monitoring equipment and grid configuration see the Supporting Information S1.

In this paper we analyze the even total harmonic distortion (ETHD) of the transformer current (ETHD) instead of THD used in the standard (IEEE, 2022). This is defined in Equation 1.

$$\mathrm{ETHD} = \frac{\sqrt{\sum_{h \in E} I_h^2}}{I_1} \times 100\% \tag{1}$$

where I_h is the RMS current of the h_{th} harmonic, I_1 is the fundamental current and E is the set of even harmonic orders up to the 50th harmonic. This definition of distortion is a reliable indicator of half-cycle saturation in a transformer and has been used successfully by Rodger et al. (2020) and Crack et al. (2024).

Tank wall vibration was measured using a vibration analyzer. A Fast Fourier Transform (FFT) of the vibration displacement was measured every 5 min, with 3,200 spectral lines being captured for each sample. In addition to vibration levels, the sound levels at the transformers were measured. The microphone was set to monitor the tank acoustic noise at ten-second intervals and at a 48 kHz sampling frequency. The vibration and acoustic levels were measured near the tank side wall for T5 and T1 parallel to the Phase C winding.

2.3. Differential Magnetometer Measurements

The Differential magnetometer method (DMM) provides a reliable method for directly measuring the line current flowing in the HV powerlines connected to grounded transformers. It uses the simple principle of Biot-Savart law that describes the magnetic field generated by the DC in the power line. Placing one fluxgate magnetometer directly under the power line and simultaneously measuring the background variations in the Earth's natural magnetic field with a remote magnetometer at least 100 m away (right hand side of Figure 3) allows for the detection of the additional magnetic field generated by the line current. Taking the geometry of the circuits (e.g., the number and height of the conductors above the ground) into account, it is easy to calculate the line current during geomagnetic active periods.

One of the first uses of differential magnetometry to detect GICs was at a pipeline in Alaska by Campbell (1980). The method was later adapted for HV power lines in Finland and Brazil by Viljanen and Pirjola (1994) and Trivedi et al. (2007). Since then several systematic studies (Hübert et al., 2024; Huebert et al., 2020; Marsal

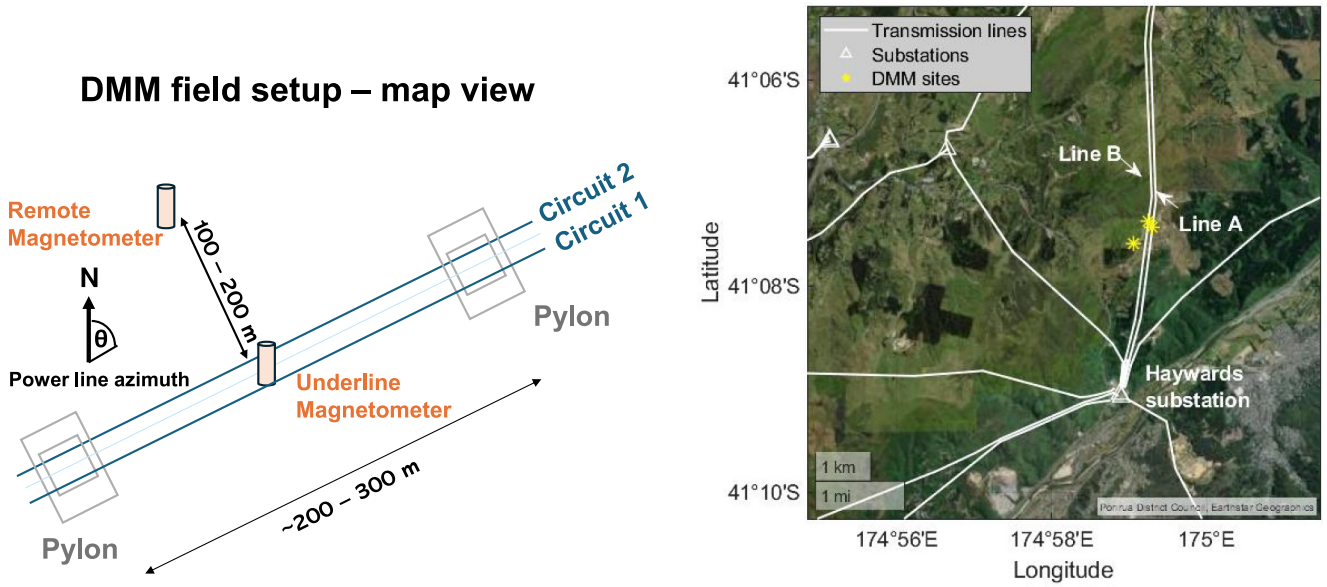

Position	Latitude	Longitude
Line A	-41.123871°	174.988279°
Line B	-41.122890°	174.987431°
remote	-41.126510°	174.984282°

Figure 3. Setup for the Differential Magnetometer Measurements. The figure to the left is the schematic diagram of the experiment, middle is the coordinates of the magnetometers and right is a map of the magnetometer locations.

et al., 2021) have shown that DMM data enable the validation of GIC models for HV power grids in combination with ground magnetic and geoelectric field data.

DMM data were collected in a location about 3 km north of Haywards substation on deforested private land (see the map shown in the right hand side of Figure 3). Three fluxgate magnetometers were installed on the site, two under the HV powerlines running from Haywards to Bunnythorpe (Line A and Line B) and one remote about 200 m away from the powerlines. Three magnetic field component data were sampled at 1s (for a detailed description see Hübert et al. (2020)).

2.4. Very Low Frequency Substation Monitoring

The technique of substation monitoring using nearby VLF receivers has been previously reported by Clilverd et al. (2018, 2020) based on observations of the Halfway Bush substation (HWB) in Dunedin, New Zealand. Evidence of harmonic distortion through enhanced odd and even AC harmonic amplitudes during GIC events of up to 50 A, associated with large geomagnetic storms in 2017 and 2018, have been observed and analyzed in detail. Typically, enhancements in the amplitude of harmonics in the 100–600 Hz range are detectable with temporal variations well correlated with changing GIC levels. The VLF observations from HWB are consistent with the idea that the local transformers radiate even harmonics of the 50 Hz fundamental mains frequency due to half-cycle saturation driven by additive DC flux produced by GIC (Boteler & Pirjola, 2017; Hayashi et al., 1978).

During the Active Injection campaign at Haywards Substation, two identical VLF receiving systems were deployed at the locations shown by the red triangles in Figure 4. Each VLF system comprised a set of orthogonal magnetic field loop aerials, a GPS receiver for timing information, a Focusrite 4i4 external sound card, and a basic laptop running Linux Ubuntu. The computer was housed in a plastic weatherproof box. The aerials were held in a vertical plane, achieving a triangular shape using a 0.9 m central mast, and guying pegs on the lower corners. An effective loop area of 11 m^2 was created by using a multi-core cable with 16 turns. A low-power preamplifier located at the base of the aerials ensured low system noise over the frequency range 100 Hz–75 kHz. The laptops ran UltraMSK software (developed in New Zealand by UltraMSK.com) which provided FFT output from 0–

Figure 4. Very low frequency (VLF) antenna installation location as denoted by the red triangles (left). Photographs of the VLF antennas, as installed in the Haywards compound (middle), and a close-up of the antenna (right).

24 kHz, with a frequency resolution of 23.4 Hz. The average amplitude for each frequency bin was logged every 4 s. The primary system operated within 200 m of the autotransformers under test and was mains powered. A second backup system operated approximately 400 m from the autotransformers and was powered by a portable battery, which was recharged each day.

3. Results

This section gives an overview of the results for the six injection tests.

3.1. Power Quality Measurements

Figure 5 shows the measurement results for the entire 9 days of testing for Haywards T1. The spikes in the DC neutral current correspond to the six injection tests.

As can be seen from the figure, the ETHD of the transformer current (an indicator of the transformer saturation) and reactive power are highly variable and appear to show little correlation to the DC neutral current measured for most of the experiment. However, due to the nature of the substation, reactive power and harmonic data are likely to be originating from a variety of sources associated with the HVDC link as well as changing customer load.

Looking closer at the data associated with the largest DC injection on 28 January, an obvious correlation between even current ETHD and injected DC is apparent (left panel of Figure 6). During the start of the injection the even ETHD increases by about 0.5% indicating an enhancement in even current harmonics. T5 was out of service on this day and showed no signs of saturation for other injection periods.

Figure 7 shows the measured DC neutral current plotted against the power quality meter-measured sixth harmonic (110 kV Side) for T1 during the entire observation period. The red curve is a second degree polynomial that represents a “best fit” for the measured data. The knee-point of the curve shows that the onset of transformer saturation is at approximately 20A of DC neutral current. This response is similar to the one observed by Clilverd et al. (2025) for similar transformers in Dunedin.

Also corresponding to the enhancement in even ETHD is the reactive power response shown in the right panel of Figure 6. This was measured from the transformers' CT and VT terminals using a power quality meter. Initially the reactive power draw jumps from about 20 MVAr to 25 MVAr at the onset of the injection with the reactive power dropping to around 23 MVAr 10 min later and fluctuating thereafter. The source of these fluctuations are not entirely due to the DC injection and likely come from a variety of sources associated with the HVDC link which makes a direct correlation between DC current and reactive power draw difficult. These observations are consistent with studies done by Dong et al. (2001) and the responses observed by Clilverd et al. (2025) on similar transformers.

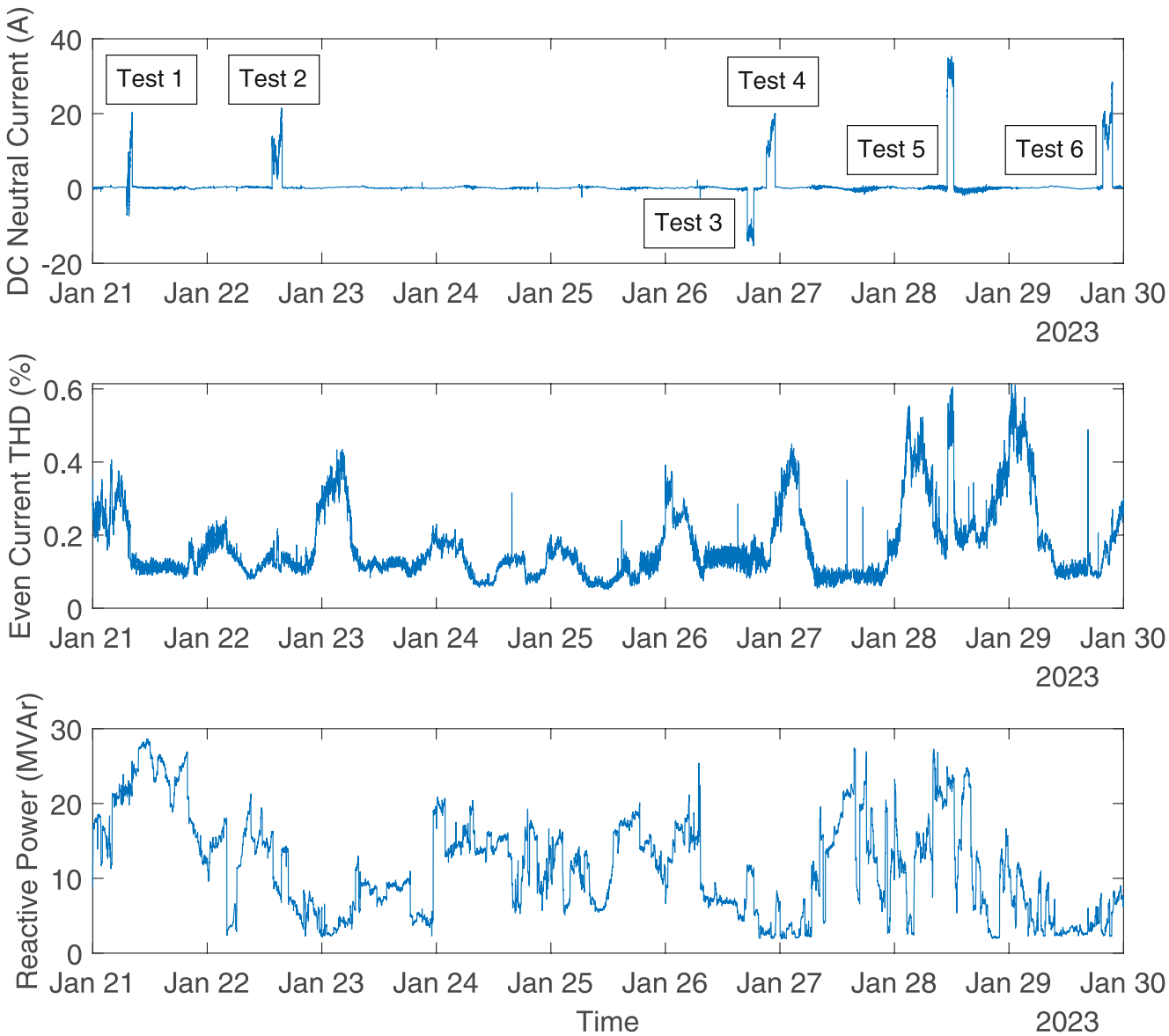

Figure 5. Transformer observations for Haywards T1 during the direct current (DC) injection campaign. The top graph is the DC Neutral Current, the middle is the Even Total Harmonic Distortion for the transformer current, and the bottom is the combined Reactive power consumption for all three phases. Time is in New Zealand Standard Time (NZST = UTC + 13 hr in summer months).

3.2. Vibration and Sound Measurements

Figure 8 shows the tank wall displacement before and during the DC injection event for Haywards T1 on the 28th of January, respectively. Before the DC injection, the peak displacement of 2.67 microns occurs at 100 Hz, corresponding to magnetostriction of the core at power frequency (R. S. Girgis & Bernesjo, 2019). After the DC injection, the vibration levels are enhanced, with the greatest relative increase being observed in the 50 Hz component. Enhancements were also observed in higher-order components up to 550 Hz. The same enhancements were observed for other injection periods albeit with lower displacement magnitude.

These results are consistent with modeling work done by Pei and Liu (2014) and R. S. Girgis and Bernesjo (2019) where the magnetostriction of the transformer core causes vibration.

Figure 9 presents the 50 Hz vibration displacement for T1 versus DC in the neutral. The data shows a relationship similar to the sixth harmonic in Figure 7. The red curve is a third degree polynomial that shows a strong

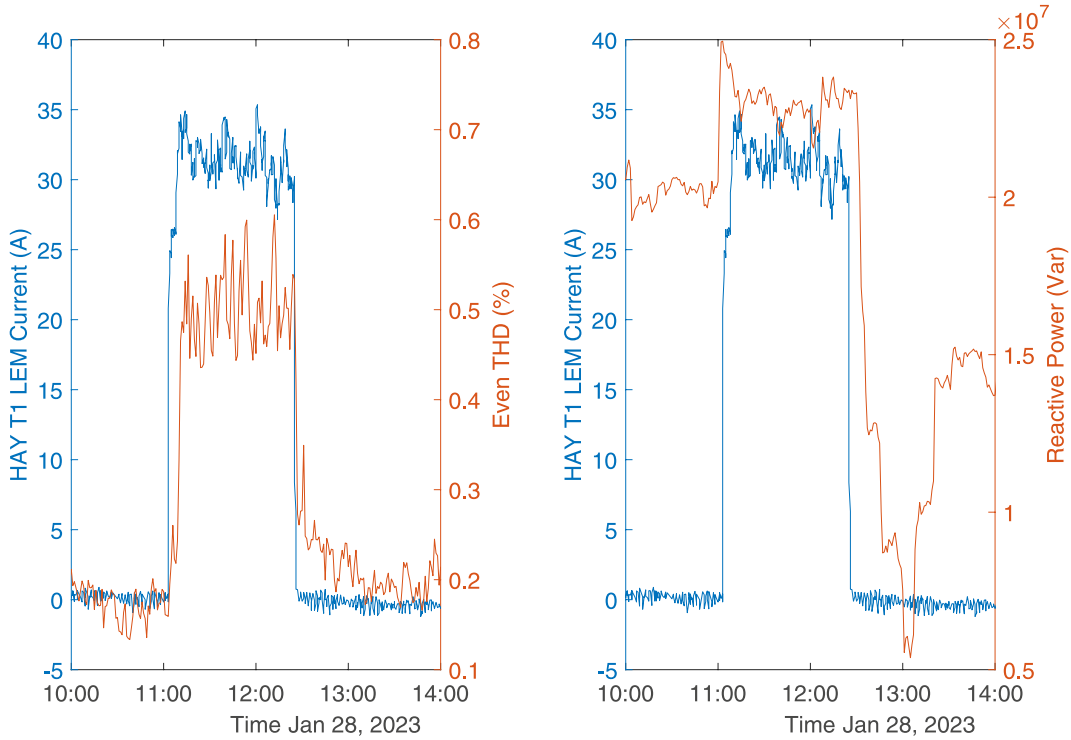

Figure 6. The graph to the left shows the direct current (DC) Neutral Current (blue) and Even Current even total harmonic distortion (orange). The graph to the right shows the DC Neutral current (blue) and the reactive power draw (orange) for Haywards T1 for the DC injection event for T1 on the 28th of January 2023 (fifth injection test).

correlation between the two variables with an R-squared value of 0.96. At the saturation knee point (20A DC) the vibration displacement also starts to saturate. Polynomial regression reveals that the quadratic and cubic terms are statistically significant ($t = 8.66$, $p = 3.0 \times 10^{-17}$ and $t = -7.70$, $p = 4.25 \times 10^{-14}$ respectively), while the linear term is not ($p = 0.76$). This indicates that the vibration response is nonlinear consistent with transformer half-cycle saturation.

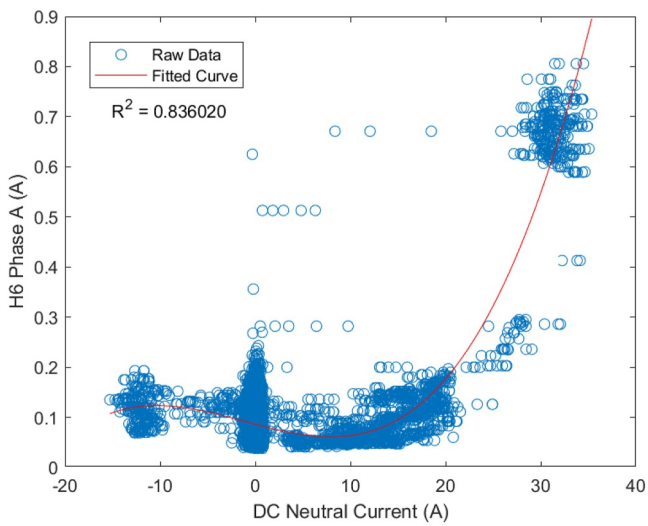

Figure 7. Sixth harmonic current versus direct current Neutral Current for Haywards T1 during the entire observation period.

Other vibration frequencies had a high correlation coefficient above 0.8 including the 150, 250, 300Hz, 350 and 450 Hz components, although they were orders of magnitude lower than seen for 50 Hz. These findings provide evidence that DC bias enhances vibration displacement and are consistent with the studies of He et al. (2012), R. S. Girgis and Bernesjo (2019) and Beltle and Tenbohlen (2012). The enhancement of the specific frequency components is likely due to mechanical resonances in the tank structure and the location of the vibration sensor on the tank.

Figure 10 presents the harmonic spectrum of the sound levels before the DC injection (blue line) and during deep DC injection-produced saturation (orange line). It is apparent that there is an enhancement in the frequency components during the DC injection, with particularly large increases at 350, 500, and 700 Hz. This enhancement is likely due to the enhanced vibration levels attributed to half-cycle saturation that were observed. These results are consistent with those obtained by He et al. (2012) and R. S. Girgis et al. (2019).

3.3. DMM Measurements

The magnetic field data at all three variometers are of good quality (few spikes or steps) and show the expected natural Sq daily variations (see

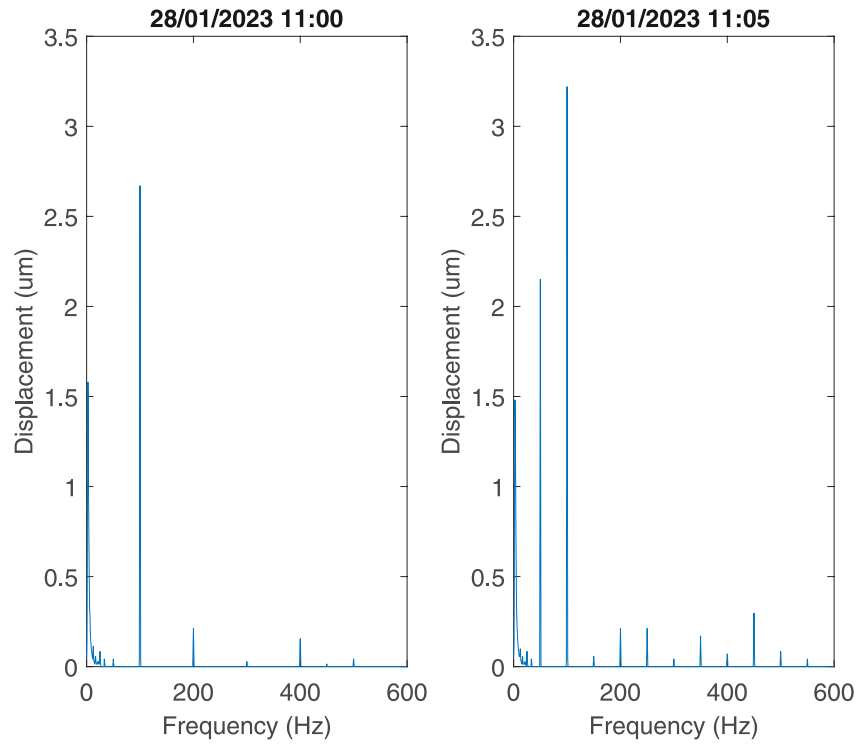

Figure 8. Vibration displacement before (left) and at the onset of (right) the direct current injection for Haywards T1.

Figure 11). Some drift in the first day of the recording is seen in the remote and the Line A data and is attributed to the box holding the instrument settling into the ground. The readings under Line A (green traces in Figure 11) show more spikes due to a closer location to the gravel road which was used by locals (collecting firewood). Large signals in the range of several hundred nT can be seen in the east-west component of the magnetic field (perpendicular to the azimuth of the powerlines) under Line A and B on 21, 22, 26, 28, and 29 January 2023, coinciding with the tests at Haywards.

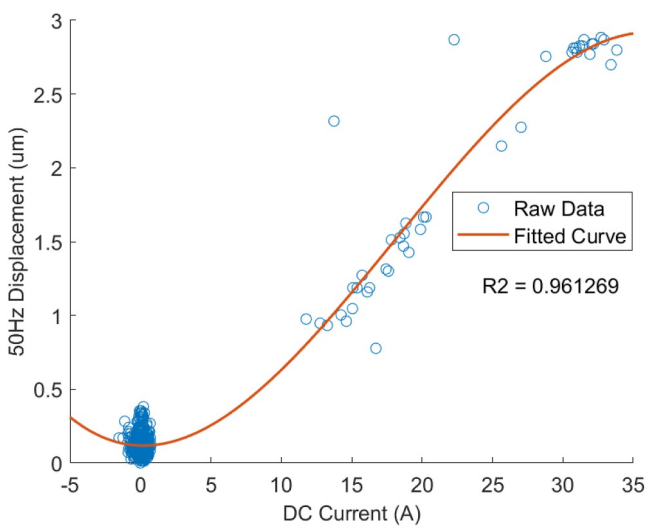

Figure 9. 50 Hz displacement component versus direct current Neutral current for T1.

From the magnetic time-series, the line currents in Line A and B were calculated during the experimentation phase according to the methodology outlined in Hübert et al. (2020). One example can be seen in Figure 12 for the injection test on 22 January. The computed line currents in Line A and B (blue and black curve) compare well to the transformer neutral measurements in transformer T1 and T5 (red and purple lines). The recorded transformer currents at substation Bunnythorpe show an inverted signal shape (yellow lines). Onset, decay and variations in the signals during the two-hour window when DC currents were injected into the Haywards station ground are very similar. Maximum line currents in both Line A and B reach 15 A, while the transformer neutral currents peak at 21 A. The different amplitudes in line and ground GICs can be explained with some of the injected current flowing through the transformers being distributed into the other lower voltage lines connected to T1 and T5.

Overall, the correlation between the two data sets (line and ground GICs) during the Transpower transformer stress tests in January 2023 illustrate that DMM data captures the DC currents affecting substation transformers. In countries where substation GIC data are not available, DMM data are an effective measure of GICs caused by geoelectric fields.

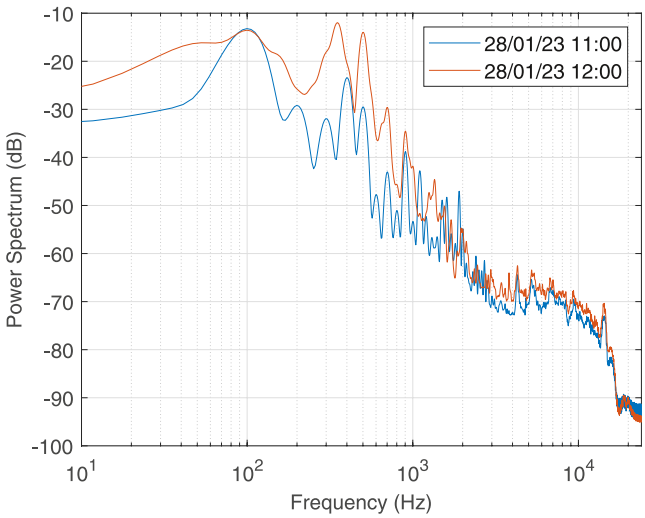

Figure 10. Sound pressure spectrum for T1 before (blue) and during (orange) the direct current injection.

3.4. VLF Measurements

Preliminary results from the VLF harmonic data suggest that observed variations in amplitude in the 100–600 Hz frequency range were correlated with temporal variations in the injected substation Earth currents provided by the HVDC connection. The HVDC transmission system generates mains frequency harmonics associated with its AC converter rectifiers. The harmonic levels are mitigated through AC harmonic filters (Miller and Dewe (1994)). At Haywards seven AC harmonic high pass filters are present on the 220 kV line, and two on the 110 kV line. Each of these switch in and out automatically. We find that, for Haywards substation, it is important to consider the operation of conditioning filter systems acting on the 110 and 220 kV lines. These filters are tuned to operate in the frequency range of 250–1,200 Hz and their effect can be clearly seen in the 0–24 kHz wideband VLF data. VLF sixth harmonic variations showed high correlation with injected HVDC current levels when two particular filters were on - both triple tuned to 550/650/1,200 Hz. We note here that no changes in filter configuration occurred during the event on the 28th of January shown in Figure 13, both key filters mentioned above were on.

The sixth harmonic amplitude variations on 28th January are shown in Figure 13. There was initially a slow increase in harmonic intensity, beginning at the time of the injection onset. This is probably due to the characteristic response time of the AC harmonic filters. After 15 min, for injected substation Earth currents ranging from 300–600 A even small variations of the order of 10s of amperes appeared to be well correlated with the VLF amplitude variations of even order harmonics. At the end of the test periods, rapid VLF amplitude decreases were observed as the injected current was switched off, with some obvious decay time exhibited between the current and the VLF amplitudes.

In comparison with the VLF observations of geomagnetic disturbance effects made at HWB in Dunedin, the VLF observations made at Haywards substation in Wellington exhibit sudden amplitude variations as AC harmonic filters are switched on and off as part of the HVDC operation and its conversion to AC, and it is difficult to determine where the harmonic signals that the VLF system picks up are coming from in a large, complex substation yard. The VLF observations are consequently significantly more complex to analyze than those published from Halfway Bush in Dunedin (Clilverd et al. (2018, 2020)).

4. Discussion

For the transformer monitoring clear evidence of half-cycle saturation was found during the test on the 28th of January where 35 A of DC current flowed in Haywards T1. Enhancements in the even order current harmonics were found alongside increased vibration and sound levels. The saturation knee-point was found to be around 20 Amps DC. This result is significant as the transformer is of three-phase three-limb core construction which is assumed to be relatively resilient to GIC (Rezaei-Zare et al., 2016). If the transformers were of shell form or single-phase construction, we would expect to see much higher levels of half-cycle saturation and a lower saturation knee-point.

These results are also consistent with research done by Clilverd et al. (2025) which analyzed transformer responses in Dunedin New Zealand during the Gannon Storm. Two transformers of similar size and construction at Half-Way Bush substation exhibited similar responses to Haywards with the saturation threshold of around 25–35 ADC. The transformers started to exhibit a reactive power response after around 30 ADC at 0.038 MVAr/A for T6 and 0.026 MVAr/A for T3. DC current levels only exceeded 30 A for a short period during this experiment only reaching a peak of 35 A, which would explain why the reactive power response was not significant enough to be of concern. We note that at higher levels of DC current/GIC the reactive power response could become significant enough to be of concern to New Zealand's grid operator Transpower. We note that in the Gannon storm, significantly higher levels of GIC have been recorded of 113 A for T6 and 93 A for T3 which is well above the 30A threshold. Grid operators need to be aware of this issue as the long held assumption that core type, three-limb transformers are completely resilient to GIC is not entirely true.

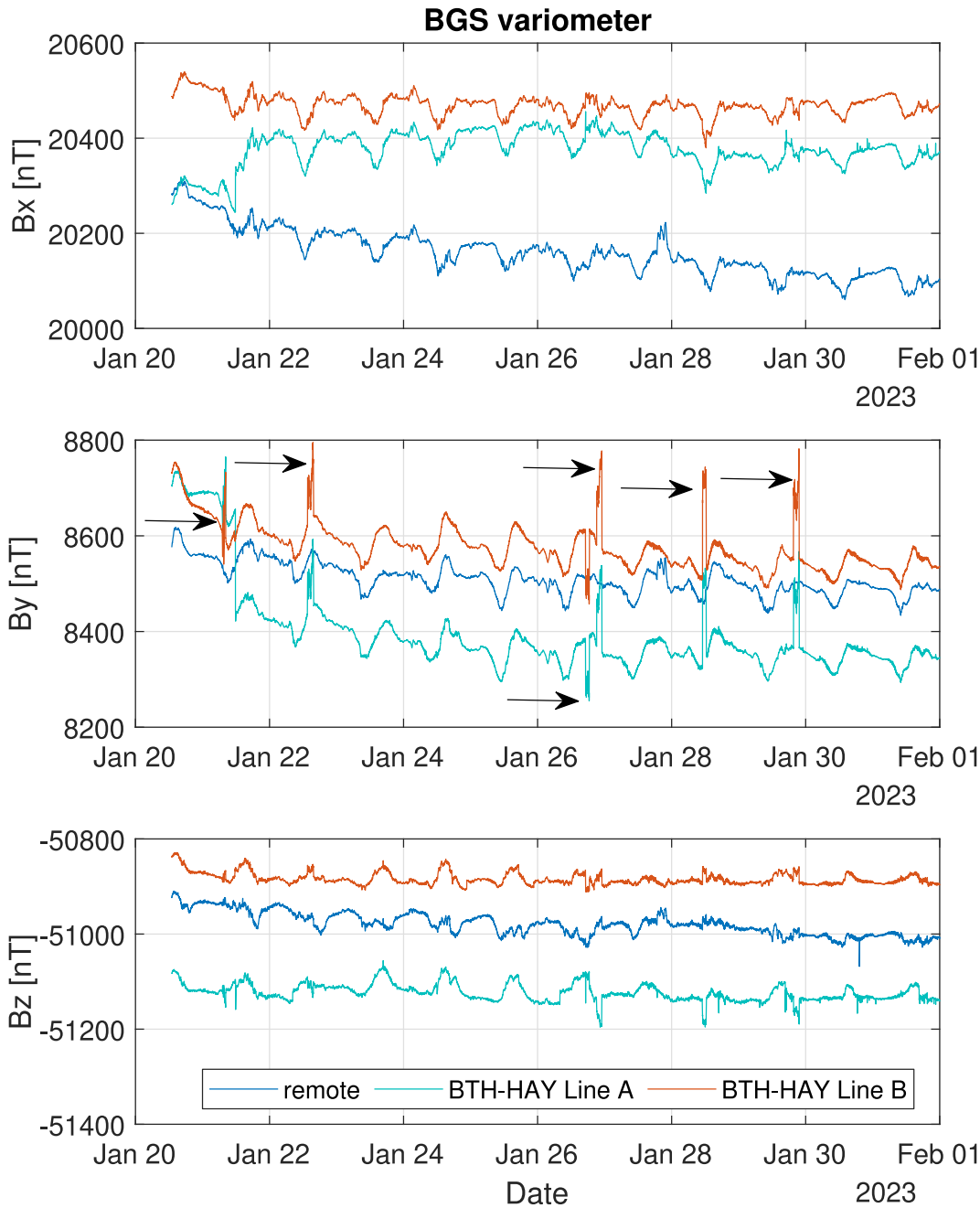

Figure 11. Three component magnetic field data during the Transformer Stress Test in January 2023. Bx–North–South component, By–East–West component, Bz–vertical component of the magnetic field. The data were measured at three installations (Blue line–"remote" site, teal–under HV line A Bunnythorpe-Haywards, orange line–under HV line B Bunnythorpe-Haywards). The East-West component of the magnetic field contains the signal from the direct current injected current (indicated with arrows) because the HV lines are running North-South.

The increase in sound and vibration levels could be significant for transformers close to urban areas where noise management needs to be considered. Vibration and sound monitoring can also be employed as another method of monitoring transformer saturation when harmonic measurements are unavailable. An example of this is demonstrated by Beltle and Tenbohlen (2012).

There was good agreement between the DMM measurements and the Autotransformer DC measurements. The line currents determined were within the range of 10–20 A, which aligns well with the naturally occurring GICs.

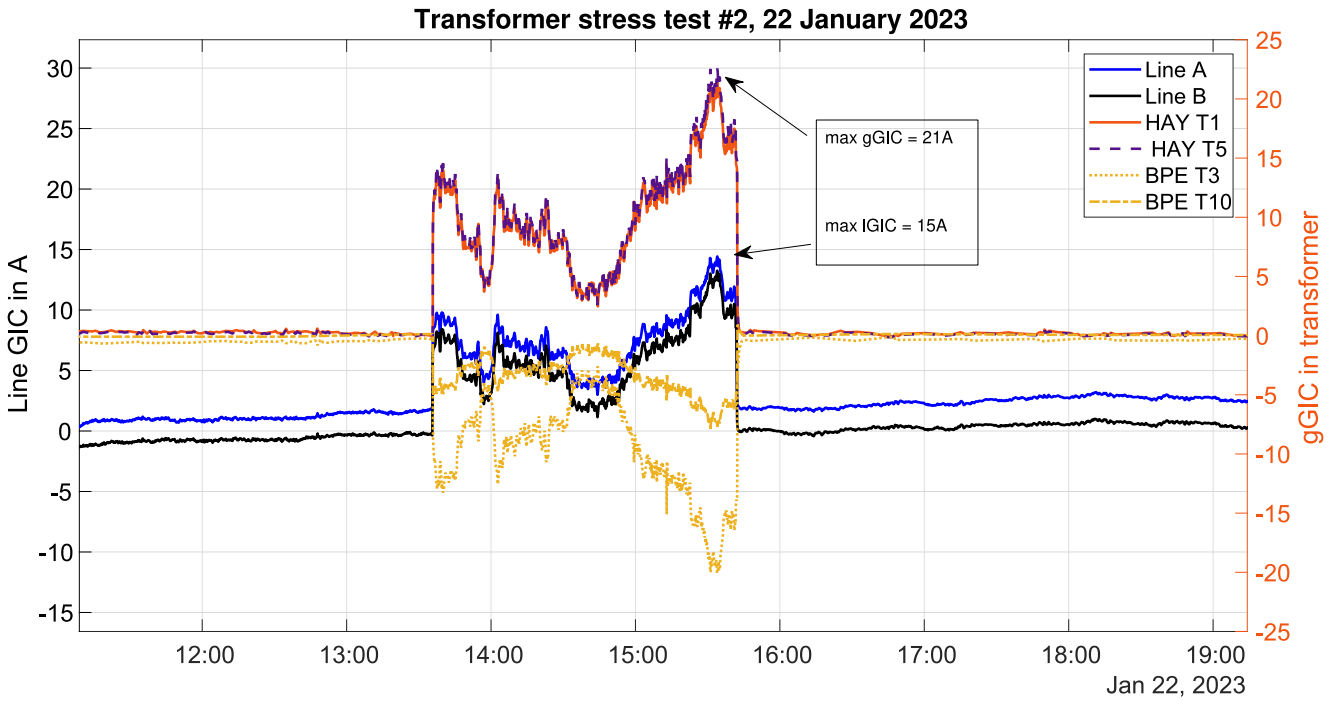

Figure 12. Line and neutral-ground GICs as measured by DMM systems under the lines A and B and in the transformers at substations Haywards and Bunnythorpe. Ground GIC data courtesy of Transpower. The transformers in the second substation show an inverted signal shape, due to the current flowing in the opposite direction.

The measured DC exhibits a strong correlation with the documented line current. It also indicated that the DC flowed North out of the station rather than south to Benmore.

The VLF observations conducted at Haywards substation in Wellington display greater abrupt changes in amplitude compared to the VLF observations at HWB in Dunedin, making their analysis more intricate. When studying Haywards substation, it is crucial to take into account the functioning of conditioning filter systems installed on the 110 and 220 kV lines. These filters are specifically designed to operate within the frequency range of 250–1,200 Hz, and their impact is evident in the wideband VLF data spanning from 0 to 24 kHz.

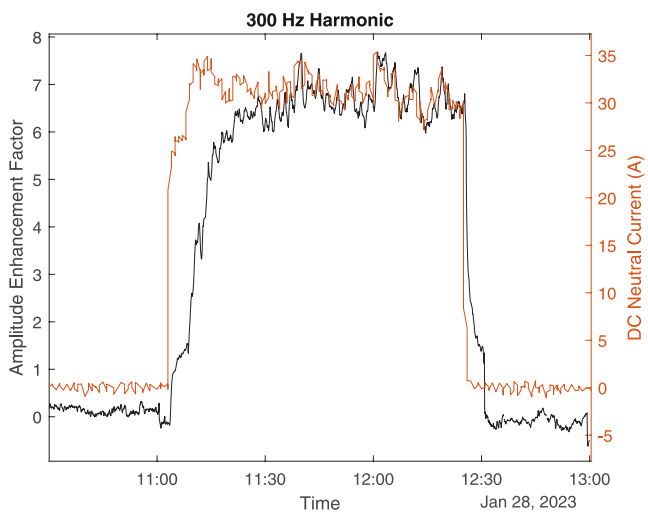

Figure 13. Very low frequency measured sixth harmonic amplitude variations and direct current Neutral current on the 28th of January 2023. Time is in New Zealand Standard Time (NZST = UTC + 13 hr in summer months).

The three different measurement methods all show results that are consistent with each other, where the current harmonics in the transformer align with the observed VLF observations (when the conditioning filters are taken into account). DMM measurements align well with the measured DC and can be a reliable proxy for measuring GIC when direct measurements are not available. DMM can also be a useful tool for measuring line GICs which can be important for protection and for monitoring the distribution and direction of GIC in a power network.

In summary the experiment provided valuable insights into the impact of GICs on in-service equipment including:

- The saturation characteristics of GIC on in-service power transformers.
- Even THD shows good correlation with half-cycle saturation. This is valuable for monitoring transformers during geomagnetic disturbances, particularly in light of the New Zealand wide even ETHD changes seen during such disturbances (e.g.., Rodger et al. (2020); Crack et al. (2024))
- Transformers can experience enhanced vibration and sound levels when experiencing DC currents. This could be an issue for transformers close to urban areas where noise management needs to be considered.

- DC Current measurements show excellent correlation with DMM measurements. This provides a reliable proxy for GIC when direct measurements are not available or can be useful for monitoring line GICs.
- VLF harmonic measurements correlate well with power quality harmonic measurements when the operation of the filter banks are taken into account.
- Three-Phase Three-Limb power transformers typically assumed to be immune to GIC can undergo half-cycle saturation at higher GIC levels than shell form transformers.

The lessons learned from this study can be applied to power systems vulnerable to GIC. These monitoring methods can be particularly important for informing on GIC mitigation plans which some power system operators are starting to implement. For example, Transpower has taken cautionary steps to protect transformers in the grid from GIC with a geomagnetic storm mitigation plan as described by (Mac Manus et al., 2023).

5. Conclusions

In conclusion, six DC injection tests were performed using the HVDC link at Haywards substation. The purpose of the experiment was to measure the effects of GIC on in-service power transformers. Evidence of half-cycle saturation was found during the test on the 28th of January where 35 A of DC current flowed in Haywards T1. Enhancements in the even harmonics were found alongside increased vibration and sound levels and the VLF observations correlated well with the current harmonics. Overall this experiment provides a good insight into the effects of GIC on power transformers and their monitoring methods.

Conflict of Interest

The authors declare no conflicts of interest relevant to this study.

Availability Statement

The DMM, VLF and Transformer measurements are available from the University of Canterbury Data Repository (Lapthorn, 2025). The MATLAB scripts used to reproduce the figures are available from Zenodo (Subritzky, 2025). The vibration measurements were analyzed using an excel workbook by the manufacturer RION. This can be obtained from the manufacturers website (RION, 2022). Note that an account needs to be registered for access.

Acknowledgments
This research was supported by the New Zealand Ministry of Business, Innovation and Employment Endeavour Fund Research Programme contract UOOX2002. The author would like to thank Transpower New Zealand for the grid data and diagrams and the landowners along Mt Cecil Road for access permission to take the DMM measurements. Open access publishing facilitated by University of Canterbury, as part of the Wiley - University of Canterbury agreement via the Council of Australasian University Librarians

References

Beltle, M., & Tenbohlen, S. (2012). Usability of vibration measurement for power transformer diagnosis and monitoring. In *2012 IEEE international conference on condition monitoring and diagnosis* (pp. 281–284). https://doi.org/10.1109/CMD.2012.6416431

Bolduc, L. (2002). GIC observations and studies in the hydro-Québec power system. *Journal of Atmospheric and Solar-Terrestrial Physics*, *64*(16), 1793–1802. https://doi.org/10.1016/S1364-6826(02)00128-1

Boteler, D. H. (2019). A 21st century view of the March 1989 magnetic storm. *Space Weather*, *17*(10), 1427–1441. https://doi.org/10.1029/2019SW002278

Boteler, D. H., & Pirjola, R. J. (2017). Modeling geomagnetically induced currents. *Space Weather*, *15*(1), 258–276. https://doi.org/10.1002/2016SW001499

Campbell, W. H. (1980). Observation of electric currents in the Alaska oil pipeline resulting from auroral electrojet current sources. *Geophysical Journal International*, *61*(2), 437–449. https://doi.org/10.1111/j.1365-246X.1980.tb04325.x

Clilverd, M. A., Rodger, C. J., Brundell, J. B., Dalzell, M., Martin, I., Mac Manus, D. H., & Thomson, N. R. (2020). Geomagnetically induced currents and harmonic distortion: High time resolution case studies. *Space Weather*, *18*(10), e2020SW002594. https://doi.org/10.1029/2020SW002594

Clilverd, M. A., Rodger, C. J., Brundell, J. B., Dalzell, M., Martin, I., Mac Manus, D. H., et al. (2018). Long-lasting geomagnetically induced currents and harmonic distortion observed in New Zealand during the 7–8 September 2017 disturbed period. *Space Weather*, *16*(6), 704–717. https://doi.org/10.1029/2018SW001822

Clilverd, M. A., Rodger, C. J., Manus, D. H. M., Brundell, J. B., Dalzell, M., Renton, A., et al. (2025). Geomagnetically induced currents, transformer harmonics, and reactive power impacts of the gannon storm in May 2024. *Space Weather*, *23*(4), e2024SW004235. https://doi.org/10.1029/2024SW004235

Crack, M., Rodger, C. J., Clilverd, M. A., Mac Manus, D. H., Martin, I., Dalzell, M., et al. (2024). Even-order harmonic distortion observations during multiple geomagnetic disturbances: Investigation from New Zealand. *Space Weather*, *22*(5), e2024SW003879. https://doi.org/10.1029/2024SW003879

Dong, X., Liu, Y., & Kappenman, J. (2001). Comparative analysis of exciting current harmonics and reactive power consumption from gic saturated transformers. 318–322. https://doi.org/10.1109/PESW.2001.917055

Erinmez, I., Kappenman, J. G., & Radasky, W. A. (2002). Management of the geomagnetically induced current risks on the national grid company's electric power transmission system. *Journal of Atmospheric and Solar-Terrestrial Physics*, *64*(5), 743–756. https://doi.org/10.1016/S1364-6826(02)00036-6

Ferguson, R., Wilkinson, W., & Hill, R. (2000). Electricity use and economic development. *Energy Policy*, *28*(13), 923–934. https://doi.org/10.1016/S0301-4215(00)00081-1

Girgis, R., & Ko, C.-D. (1992). Calculation techniques and results of effects of GIC currents as applied to large power transformers. *IEEE Transactions on Power Delivery*, *7*(2), 699–705. https://doi.org/10.1109/61.127070

Girgis, R., & Vedante, K. (2012). Effects of GIC on power transformers and power systems. In *Pes T&D 2012* (pp. 1–8). https://doi.org/10.1109/TDC.2012.6281595

Girgis, R., & Vedante, K. (2013). Methodology for evaluating the impact of GIC and GIC capability of power transformer designs. In *2013 IEEE power and energy society general meeting* (pp. 1–5). https://doi.org/10.1109/PESMG.2013.6672911

Girgis, R. S., Bernesjo, M. S., Hodgdon, S., DeMay, J., Arritt, B., & Van Der Zel, L. (2019). Experience with impact of GIC on noise performance of large power transformers. In *2019 IEEE power and energy society general meeting (PESGM)* (pp. 1–5). https://doi.org/10.1109/PESGM40551.2019.8973439

Girgis, R. S., & Bernesjo, M. S. (2019). Magnitudes and characteristics of tank vibrations of power transformers. In *2019 IEEE power and energy society general meeting (PESGM)* (pp. 1–5). https://doi.org/10.1109/PESGM40551.2019.8973992

Hayashi, K., Oguti, T., Watanabe, T., Tsuruda, K., Kokubun, S., & Horita, R. E. (1978). Power harmonic radiation enhancement during the sudden commencement of a magnetic storm. *Nature*, *275*(5681), 627–629. https://doi.org/10.1038/275627a0

He, J., Yu, Z., Zeng, R., & Zhang, B. (2012). Vibration and audible noise characteristics of AC transformer caused by HVDC system under monopole operation. *IEEE Transactions on Power Delivery*, *27*(4), 1835–1842. https://doi.org/10.1109/TPWRD.2012.2205409

Hübert, J., Beggan, C. D., Richardson, G. S., Gomez-Perez, N., Collins, A., & Thomson, A. W. P. (2024). Validating a UK geomagnetically induced current model using differential magnetometer measurements. *Space Weather*, *22*(2), e2023SW003769. https://doi.org/10.1029/2023SW003769

Hübert, J., Beggan, C. D., Richardson, G. S., Martyn, T., & Thomson, A. W. P. (2020). Differential magnetometer measurements of geomagnetically induced currents in a complex high voltage network. *Space Weather*, *18*(4), e2019SW002421. https://doi.org/10.1029/2019SW002421

Huebert, J., Beggan, C. D., Richardson, G. S., & Thomson, A. W. P. (2020). Utilizing magnetotelluric and differential magnetometer measurements for the validation of geomagnetically induced current models in a complex power network. In *Egu general assembly conference abstracts*. https://doi.org/10.5194/egusphere-egu2020-8374.8374

IEEE. (2022). IEEE standard for harmonic control in electric power systems. *IEEE Std 519-2022 (Revision of IEEE Std 519-2014)*, 1–31. https://doi.org/10.1109/IEEESTD.2022.9848440

IEEE. (2024). IEEE guide for establishing power transformer capability while under geomagnetic disturbances. *IEEE Std C57.163-2023 (Revision of IEEE Std C57.163-2015)*, 1–56. https://doi.org/10.1109/IEEESTD.2023.10431702

Lapthorn, A. (2025). Haywards DC injection testing–Jan 2023 (version 1) [Dataset]. *University of Canterbury Data Repository*. https://doi.org/10.26021/canterburynz.29835422.v1

Mac Manus, D. H., Rodger, C. J., Dalzell, M., Thomson, A. W. P., Clilverd, M. A., Petersen, T., et al. (2017). Long-term geomagnetically induced current observations in New Zealand: Earth return corrections and geomagnetic field driver. *Space Weather*, *15*(8), 1020–1038. https://doi.org/10.1002/2017SW001635

Mac Manus, D. H., Rodger, C. J., Renton, A., Ronald, J., Harper, D., Taylor, C., et al. (2023). Geomagnetically induced current mitigation in New Zealand: Operational mitigation method development with industry input. *Space Weather*, *21*(11), e2023SW003533. https://doi.org/10.1029/2023SW003533

Marsal, S., Torta, J. M., Curto, J. J., Canillas-Pérez, V., Cid, O., Ibañez, M., & Marcuello, A. (2021). Validating GIC modeling in the Spanish power grid by differential magnetometry. *Space Weather*, *19*(12), e2021SW002905. https://doi.org/10.1029/2021SW002905

Miller, A., & Dewe, M. (1994). Harmonic measurements made on the upgraded New Zealand inter-island hvdc transmission system. *IEEE Transactions on Power Delivery*, *9*(3), 1281–1288. https://doi.org/10.1109/61.311154

Newman, D. E., Carreras, B. A., Lynch, V. E., & Dobson, I. (2011). Exploring complex systems aspects of blackout risk and mitigation. *IEEE Transactions on Reliability*, *60*(1), 134–143. https://doi.org/10.1109/TR.2011.2104711

Ngwira, C. M., Pulkkinen, A., Leila Mays, M., Kuznetsova, M. M., Galvin, A., Simunac, K., et al. (2013). Simulation of the 23 July 2012 extreme space weather event: What if this extremely rare cme was earth directed? *Space Weather*, *11*(12), 671–679. https://doi.org/10.1002/2013sw000990

Pei, X. R., & Liu, L. G. (2014). Study on the characteristics of low-frequency vibration of the core of single phase transformer set caused by GIC. *Applied Mechanics and Materials*, *716–717*, 1162–1167. https://doi.org/10.4028/www.scientific.net/AMM.716-717.1162

Pulkkinen, A., Lindahl, S., Viljanen, A., & Pirjola, R. (2005). Geomagnetic storm of 29–31 October 2003: Geomagnetically induced currents and their relation to problems in the Swedish high-voltage power transmission system. *Space Weather*, *3*(8). https://doi.org/10.1029/2004SW000123

Rezaei-Zare, A., Marti, L., Narang, A., & Yan, A. (2016). Analysis of three-phase transformer response due to GIC using an advanced duality-based model. *IEEE Transactions on Power Delivery*, *31*(5), 2342–2350. https://doi.org/10.1109/TPWRD.2015.2505499

RION. (2022). VA-12 excel workbook VA12.xlsm for presentation of VA-12 data (version 1.2.0) [Software]. *RION CO., LTD*. Retrieved from https://rion-sv.com/download/software/1087177.html

Rodger, C. J., Clilverd, M. A., Mac Manus, D. H., Martin, I., Dalzell, M., Brundell, J. B., et al. (2020). Geomagnetically induced currents and harmonic distortion: Storm-time observations from New Zealand. *Space Weather*, *18*(3), e2019SW002387. https://doi.org/10.1029/2019SW002387

Subritzky, S. (2025). sps55/haywards-dc-injection: Haywards DC injection (version 1.0.0) [Software]. *Zenodo*. https://doi.org/10.5281/zenodo.16921987

Teh, X. Y., Xue, Y., Liang, Z., Ramirez, J., & Lapthorn, A. (2022). Investigation of geomagnetically induced currents (GICs) susceptibility of different three-phase power transformer cores. In *2022 7th IEEE workshop on the electronic grid (eGRID)* (pp. 1–5). https://doi.org/10.1109/eGRID57376.2022.9990010

Trivedi, N. B., Vitorello, I., Kabata, W., Dutra, S. L. G., Padilha, A. L., Bologna, M. S., et al. (2007). Geomagnetically induced currents in an electric power transmission system at low latitudes in Brazil: A case study. *Space Weather*, *5*(4). https://doi.org/10.1029/2006SW000282

Tsurutani, B. T., Gonzalez, W. D., Lakhina, G. S., & Alex, S. (2003). The extreme magnetic storm of 1–2 September 1859. *Journal of Geophysical Research*, *108*(A7). https://doi.org/10.1029/2002JA009504

Viljanen, A., & Pirjola, R. (1994). Geomagnetically induced currents in the Finnish high-voltage power system. *Surveys in Geophysics*, *15*(4), 383–408. https://doi.org/10.1007/BF00665999

Yamashita, K., Joo, S.-K., Li, J., Zhang, P., & Liu, C.-C. (2008). Analysis, control, and economic impact assessment of major blackout events. *European Transactions on Electrical Power*, *18*(8), 854–871. https://doi.org/10.1002/etep.304

Zeng, R., Yu, Z., He, J., Zhang, B., & Niu, B. (2011). Study on restraining DC neutral current of transformer during HVDC monopolar operation. *IEEE Transactions on Power Delivery*, *26*(4), 2785–2791. https://doi.org/10.1109/TPWRD.2011.2161345